Laser ablated sub-wavelength structure anti-reflection coating on an alumina lens

Shaul Hanany^a, Scott Cray^a, Jan Düsing^b, Calvin Firth^a, Jürgen Koch^b, Kuniaki Konishi^c, Rex Lam^a, Tomotake Matsumura^{d,e,f}, Haruyuki Sakurai^c, Yuki Sakurai^{d,g,h}, Aritoki Suzukiⁱ, Ryota Takaku^{d,j}, Qi Wen^a, Alexander Wienke^b, and Andrew Y. Yan^a

^aSchool of Physics and Astronomy, University of Minnesota, Twin Cities, 115 Union St. SE, Minneapolis MN 55455, USA

^bLaser Zentrum Hannover, Hollerithallee 8 D-30419, Hannover, Germany ^cInstitute for Photon Science and Technology (IPST), The University of Tokyo, 7-3-1 Hongo, Bunkyo-ku, Tokyo 113-8654, Japan

^dKavli Institute for the Physics and Mathematics of the Universe (IPMU), The University of Tokyo, 5-1-5 Kashiwa-no-Ha, Kashiwa, Chiba 277-8583, Japan

^eCenter for Data Driven Discovery (CD3), Kavli Institute for the Physics and Mathematics of the Universe (IPMU), The University of Tokyo, 5-1-5 Kashiwa-no-Ha, Kashiwa, Chiba 277-8583, Japan

^fILANCE, CNRS, University of Tokyo International Research Laboratory, Kashiwa, Chiba 277-8582, Japan

gOkayama University, 3-1-1 Tsushimanaka Kita-ku, Okayama, Japan
hSuwa University of Science, 5000-1 Toyohira, Chino-shi, Nagano 391-0292, Japan
iLawrence Berkeley Laboratory, 1 Cyclotron Road, Berkeley, CA 94720-8235, USA
jInter-University Research Institute Cooperation High Accelerator Research Organization (KEK) International Center for Quantum-field Measurement Systems for Studies of the Universe and Particles (QUP), 1-1, Oho, Tsukuba, Ibaraki, 305-0801, Japan

ABSTRACT

We used laser ablation to fabricate sub-wavelength structure anti-reflection coating (SWS-ARC) on a 5 cm diameter alumina lens. With an aspect ratio of 2.5, the SWS-ARC are designed to give a broad-band low reflectance response between 110 and 290 GHz. SWS shape measurements give 303 µm pitch and total height between 750 and 790 µm height, matching or exceeding the aspect ratio design values. Millimeter-wave transmittance measurements in a band between 140 and 260 GHz show the increase in transmittance expected with the ARC when compared to finite element analysis electromagnetic simulations. To our knowledge, this is the first demonstration of SWS-ARC on an alumina lens, opening the path for implementing the technique for larger diameter lenses.

Keywords: Alumina, Anti-Reflection Coating, Sub-Wavelength Structures, Millimeter-Wave Optical Components

1. INTRODUCTION

Millimeter-wave telescopes require lenses with low absorption loss. In many instances, and specifically for the low noise measurements required for cosmic microwave background (CMB) studies, ^{1,2} the lenses are operated at low temperatures to reduce thermal load on the detectors. In these applications alumina is a desirable material. When cooled to cryogenic temperatures, 99.5% or higher purity variants give a loss tangent $\delta \simeq 0.0005$, ³ among the lowest available with non-birefringent materials. Relative to polyethylene, a material that has similar absorptive

Send correspondence to hanany@umn.edu

loss,⁴ alumina is advantageous because it has approximately two times higher index of refraction $n_{\rm alumina} \simeq 3.1$, leading to thinner optical elements. Because it has orders of magnitude higher thermal conductance,^{5,6} optical components with diameter of tens of cm attain lower and more uniform temperature distributions when heat-sunk at cryogenic temperatures.⁷ At the THz frequency band, the absorption of alumina rises more rapidly compared to polyethylene, making alumina lenses good absorbers for high frequency radiation thus obviating the need for additional filters. Alumina lenses have been implemented with several CMB instruments.⁸⁻¹⁰

Alumina's high index necessitates an anti-reflection coating (ARC) without which reflective losses could exceed 50%. Among the various approaches proposed for implementing ARC for alumina,^{3,11–14} our group has focused on fabricating sub-wavelength structures (SWS),¹⁵ which has been on occasion also called metamaterial ARC.^{16–18} Because alumina is among the hardest materials, we have been fabricating the SWS-ARC using laser ablation.^{7,19–26} Recently, we reported on the first 30 cm diameter alumina filter with SWS-ARC, which was integrated into the MUSTANG2 instrument operating with the Green Bank telescope.⁷ The measured transmission was 98% with a reflective loss of 1%, and total fabrication time of less than 4 days.⁷

To date, SWS fabricated on alumina were made on flat disks.^{7,13} In this paper we report on the first fabrication of SWS-ARC on an alumina *lens*. We discuss sample preparation in Section 2, SWS shape and lens transmission measurements in Section 3, and we discuss the results in Section 4.

2. SAMPLE PREPARATION

NTK Ceratech fabricated three identical alumina plano-spherical lenses with design specifications given in Table 1, see Figure 1. Measurements of the lens are described in Section 3. The material was A995LD, which should have 99.5% Al₂O₃. Previous samples of this material gave a measured index of refraction $n = 3.12 \pm 0.03$ (68%) and loss tangent $\delta < 4.6 \cdot 10^{-4}$ (95%).⁷ To calculate transmission and reflection in this paper we use the previously measured n and $\delta = 4 \cdot 10^{-4}$.

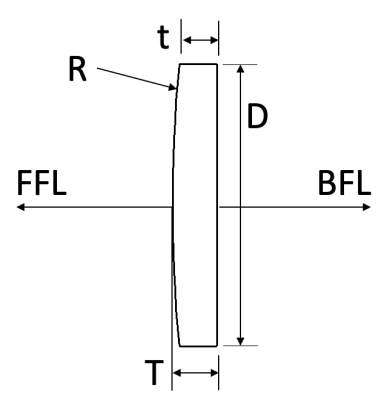


Figure 1: Sketch of the lens (not to scale). The parameters are given in Table 1.

The shape of the SWS-ARC were motivated by a design of an alumina lens for the COSMO instrument, 27 a millimeter-wave spectrometer that will be located in Antarctica and will measure the spectrum of the CMB. COSMO will operate over a band between 110 and 290 GHz and we therefore designed pyramid-shape SWS-ARC with the dimensions listed in Table 3. During the design we assume an array of square symmetric pyramids with a single depth (or height), denoted d_t . The COSMO lens will be 220 mm in diameter and 13 mm thick in its middle. To give indication of the expected performance of the SWS-ARC as a function of frequency we give in Figure 2 the predicted transmission of a flat slab of alumina that is 10 mm thick. The average reflectance at frequencies between 110 and 290 GHz is expected to be less than 2%.

The SWS were fabricated using laser ablation of v-shaped grooves in a manner similar to previous samples produced by our group.^{7,19–26,28} The parameters of the femtosecond laser are given in Table 2. There are two key differences between this fabrication and past projects: (1) this fabrication was done on a curved sample, and (2) we coordinated simultaneous continuous motion of the sample stage and the laser beam (using a laser

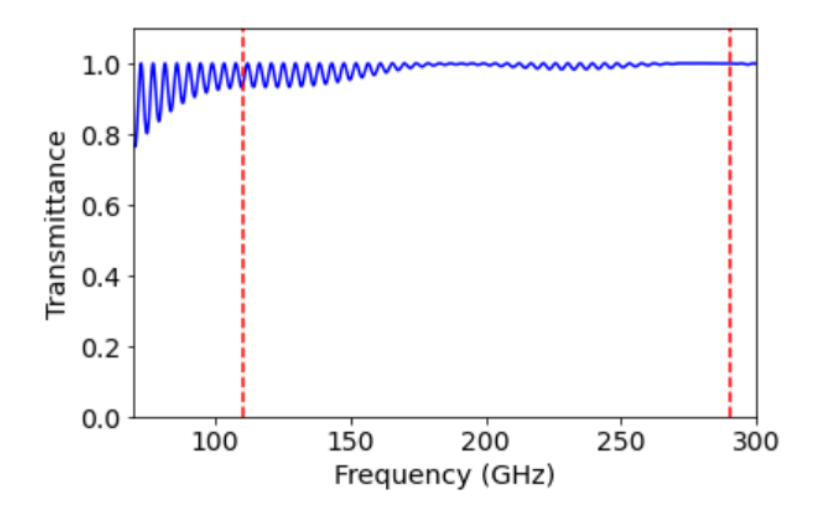


Figure 2: The expected transmission of the COSMO lens with SWS-ARC similar to the ones fabricated on the curved side of the smaller prototype lens presented in this paper. The COSMO measurement bandwidth is between 110 and 290 GHz (vertical red lines). To focus on the reflectance properties, the transmission calculation does not include loss.

	Design (mm)	Measurement (mm)		
Diameter (D)	50.00	50.06 ± 0.05		
Radius of curvature (R)	274.83	276.05^{\dagger}		
Total thickness (T)	8.00	8.10		
Disc thickness (t)	6.86	6.86		
Front focal length (FFL)	129.64	130.21		
Back focal length (BFL)	127.07	127.65		
Effective focal length	129.64	130.21		
† Least squares best fit radius of curvature.				

Table 1: Lens Parameters. The focal lengths are given in the ray limit and are derived from the radii of curvature.

scanner) over the planar x, and y dimensions. The position of the beam in z was maintained constant for both the curved and flat sides of the lens. We fabricated the SWS over a 46 mm diameter circular area in 20.7 hours.

Table 2: Laser and Process ParametersModel: Coherent Monaco 1035-80-60Wavelength1035 nmRepetition rate755 kHzPulse duration330 fsPulse energyup to $40 \mu J$ Spot diameter $(1/e^2)$ 50 μm

3. MEASUREMENTS

3.1 Shape

We measured the shape of one of the bare lenses with a coordinate measurement machine (CMM). The lens was placed on a granite table on its flat side, assumed to be an x, y plane, and the CMM was used to measure the diameter, to map the curved surface in z, and to find the best fit spherical surface. The RMS z deviations from the nominal surface were 0.01 mm. Other results of the measurements are given in Table 1. We assume all lenses have the same geometry as the one measured.

After we laser-ablated the ARC, both sides of the lens were imaged with a confocal microscope. A large 25 mm^2 and a smaller 0.35 mm^2 sections from the convex side of the lens are shown in Figure 3. They are typical of the fabrication quality over the entire lens. In five sub-areas on each side of the lens, as shown in the left panel of Figure 4, we analyzed one-dimensional profiles in x, y, and diagonally, see the middle panel in the figure, and we quantified the pyramid shape parameters, which are defined in the right panel. The average values and standard deviations for 75 pyramids in each side of the lens and in all 5 areas are given in Table 3. The array period of the pyramids, commonly called the pitch, was measured using about 20 pyramids in each of x and y profiles from higher magnification images along the horizontal strip in the center of the lens, see Figure 4.

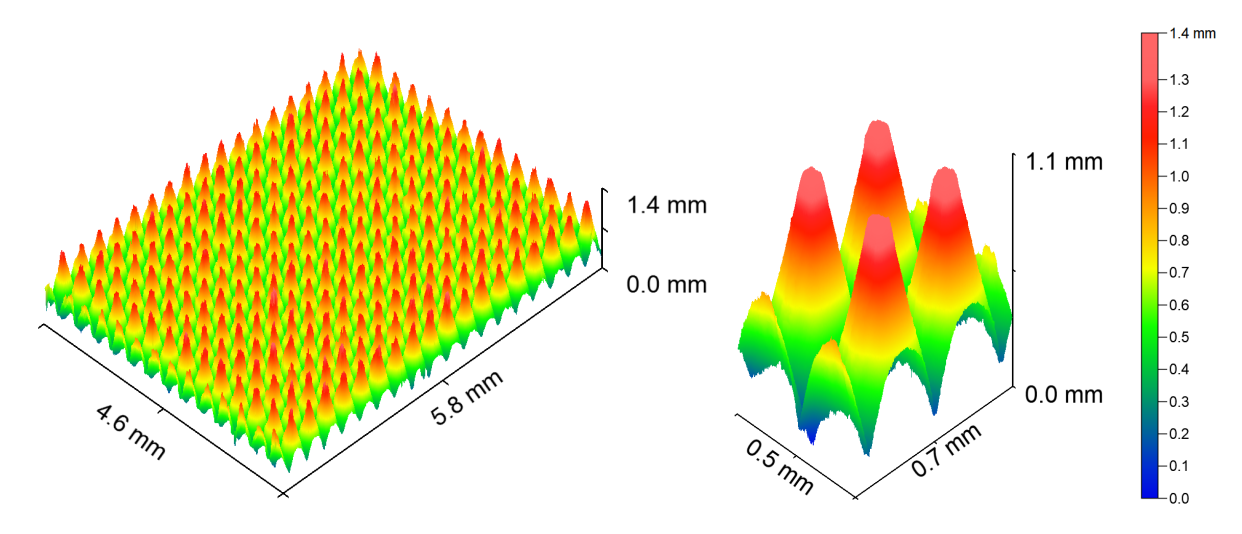


Figure 3: Confocal microscope images of the SWS-ARC from the convex side of the lens. The pyramid parameters are defined in Figure 4 and are given in Table 3.

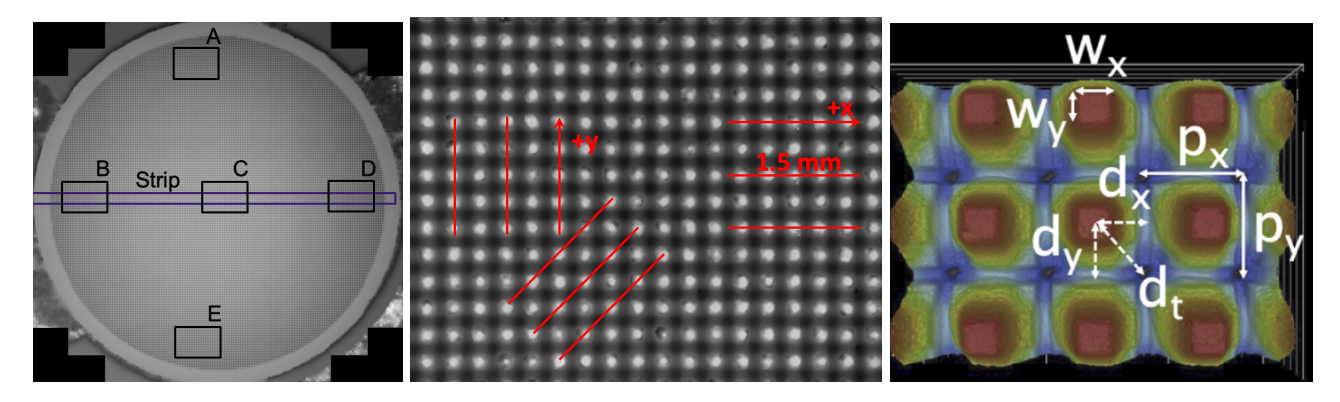


Figure 4: Left: overview of the convex side of the 5 cm diameter lens. All pyramid shape parameters except pitch were measured in 5 rectangular areas at the top (A), bottom (E), center (C) and two sides (B and D). Pitch was measured from images along a narrow strip across the middle of the lens. Measurements were conducted on both sides of the lens. Middle: Top view of an area with 17×13 pyramids showing the tips in white. In each of areas A to E (left panel), we analyzed nine one-dimensional profiles 1.2 to 1.7 mm long (red lines). Right: the one-dimensional profiles were analyzed to extract the indicated shape parameters (Figure from Takaku et al. 7)

Figure 5 shows the progression of the ablation along the curved surface of the lens. Panel (a) features three profiles along the +y direction in section A of the lens, showing the gradient along the slope of the lens. A similar gradient is observable in profiles along the +x direction in section D (panel b). However, the three profiles in the x direction in section A (panel c) do not show a gradient, instead they are each offset from each other, as expected.

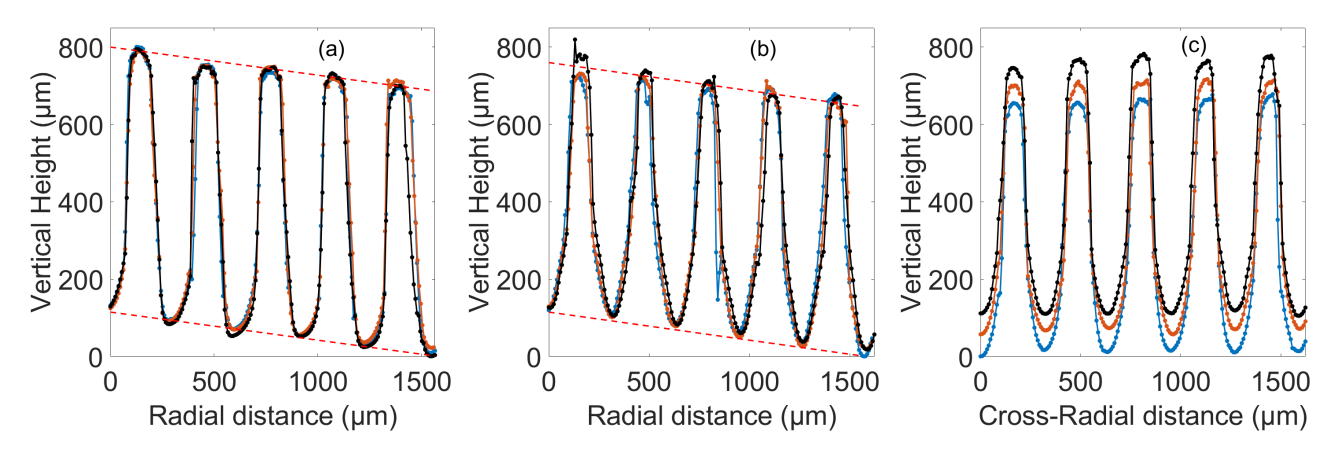


Figure 5: 1d profiles showing ablation along the sloped contour of the lens. Panels (a) and (b) are in sections A and D along +y and +x, respectively (see Figure 4), which are along an increasing radial coordinate that has an origin at the center of the lens. The *calculated* slope of the lens at the location of the profiles is overlayed (red dash) to indicate the agreement with the gradient observed with the fabricated pyramids. Panel (c) shows three +x profiles from section A, which are in cross-radial direction and therefore have no slope. They are offset from each other in the vertical direction, as expected.

	Design (µm)	Measurement (µm)	
		Convex Side	Flat Side
Pitch x (p_x)	303	303 ± 1	303 ± 1
Pitch y (p_y)	303	303 ± 1	304 ± 1
Top width x (\mathbf{w}_x)	60	60 ± 16	67 ± 12
Top width y (w_y)	60	72 ± 17	76 ± 19
Saddle depth x (d_x)	-	621 ± 35	571 ± 19
Saddle depth y (d_y)	-	661 ± 25	579 ± 17
Total depth (d_t)	750	792 ± 23	749 ± 17

Table 3: Design and measured average and standard deviation values for SWS parameters. The parameters are defined in the right panel of Figure 4.

3.2 MM-Wave Transmission

We used a vector network analyzer to measure the transmittance of the lens before and after ablating the SWS-ARC with the setup shown in Figure 6. The measurement was done at frequencies between 140 and 260 GHz with 0.25 GHz resolution. The lenses and transmitter/receiver were placed within 10 mm of the distances shown in Figure 6 and given in Table 1. Gaussian beam simulations in Zemax using the actual distances give a coupling efficiency within 1% of the efficiency at the nominal distances shown in Figure 6.

We measured transmission with two bare lenses, and with the lens closest to the receiver replaced with an AR coated lens. Each of the measurements was repeated twice to ascertain data reproducibility. The data was squared to produce a measure of power transmission, and all the subsequent analysis steps we describe refer to power. We formed the ratio of the two repeated measurements and six data points were rejected because their ratio deviated from unity by more than 33%. Most other data points were repeatable to within less than 5% percent and the standard deviation of the data, after rejection of six, was 2%.

Denoting the power counts measured with two bare lenses $T_{\rm bare}$ and the counts measured with one AR coated lens $T_{\rm 1ARC}$, we formed a ratio of the two data sets $T_{\rm ratio} \equiv T_{\rm 1ARC}/T_{\rm bare}$, which quantifies the improvement in transmission with one AR coated lens compared to none having an ARC. This ratio removes the need to normalize each of the transmission measurements, and we expect it to have values larger than 1. The ratio is sensitive to spuriously low counts $T_{\rm bare}$ and we therefore removed data that had measured $T_{\rm bare}$ less than 0.06 counts, which was 0.001% of the maximum counts over the frequency band. Most $T_{\rm bare}$ transmission data had power counts in the thousands. We also removed three data points that had $T_{\rm ratio}$ values more than 3 standard deviations from

the mean value. Figure 7 shows the ratio $T_{\rm ratio}$ as a function of frequency as well as the mean $\langle T_{\rm ratio} \rangle = 1.81$.

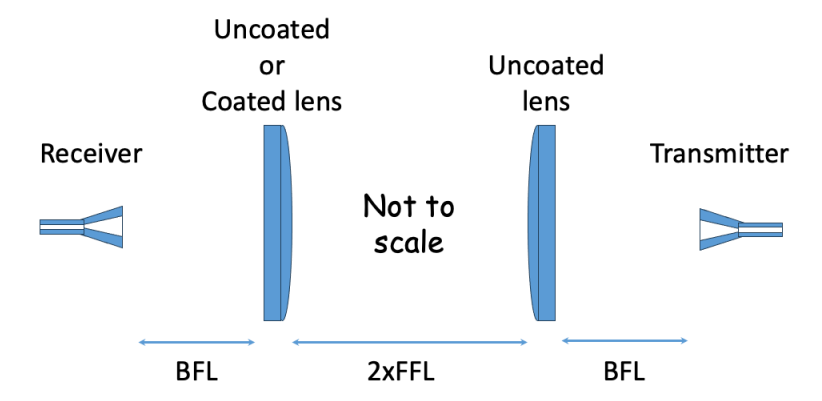


Figure 6: The experimental setup of the transmission measurements (not to scale). The actual distances between the optical elements were within 10 mm of the values given in column 'Measurement' of Table 1.

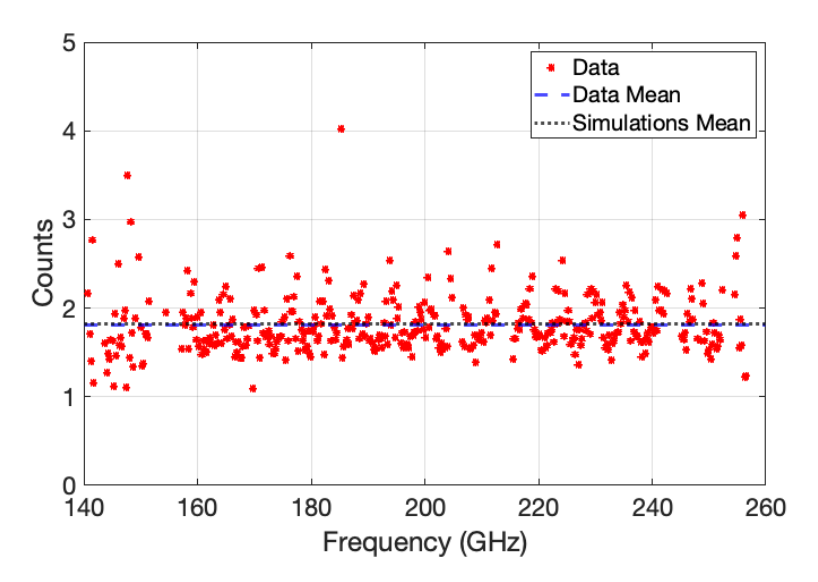


Figure 7: The ratio of transmission measurement with one coated lens to the one with two uncoated lenses $T_{\rm ratio}$ as a function of frequency (red points), the mean value of the data $\langle T_{\rm ratio} \rangle$ (blue dash), and the mean of simulated data between 100 and 140 GHz $\langle T_{\rm ratio}^{\rm sim} \rangle$ (black dot).

4. DISCUSSION AND SUMMARY

We compared the measured quantity $T_{\rm ratio}$ to the one predicted by a finite element analysis electromagnetic simulation software. The simulations required significant amount of computing resources, with every simulation taking several days to converge on a machine with 56 processors and 400 GB of RAM. Several configurations could not run because of computing resources limitations. For this reason, we scaled down the simulations in both physical size and frequency range. With the simulations we used horns placed at the foci of lenses that had only 100 mm radius of curvature, lens separation of only 10 mm, and we assessed the transmission over a frequency range between 110 and 140 GHz at a resolution of 1 GHz. Simulating the system at this frequency band is applicable because at this band we expect the average transmission of the lens to be 97%, which is only 2% lower than the average transmission at the measurement frequency band 140 - 240 GHz, see Figure 2. Simulating the system at frequencies higher than 140 GHz required more than the available computing resources.

To calculate transmission we emulated the SWS-ARC as an effective layered impedance boundary on the lens surfaces. The average of the simulated ratio over the frequency band is $\langle T_{\rm ratio}^{\rm sim} \rangle = 1.82$, nearly identical to the mean of the measured data, and it is included in Figure 7.

To our knowledge, this is the first fabrication of SWS on an alumina lens. The fabricated SWS closely resemble the design, and the measured millimeter-wave transmission gives values that are consistent with preliminary simulations, although more extensive simulations are required to ascertain complete agreement.

This work opens the path for using alumina lenses with SWS-ARC in the millimeter wavelength. Currently, up to 10 cm diameter lenses can be laser-ablated in a cost effective way, and work is ongoing to optimize the process and enable the fabrication of optical elements with tens of cm diameter.

5. ACKNOWLEDGEMENTS

We thank Nick Agladze at ITST/UC Santa Barbara for the transmission measurements. Portions of this work were conducted in the Minnesota Nano Center, which is supported by the National Science Foundation through the National Nanotechnology Coordinated Infrastructure (NNCI) under Award Number ECCS-2025124. Part of this work was supported by NSF grant number 2206087. This work was supported by JSPS KAKENHI Grant Number JP23H00107, and JSPS Core-to-Core Program, A. Advanced Research Networks. This work was performed in part at the Center for Data-Driven Discovery (CD3), Kavli IPMU (WPI). The Kavli IPMU is supported by World Premier International Research Center Initiative (WPI Initiative), MEXT, Japan. This study was funded in parts by MEXT Quantum Leap Flagship Program (MEXT Q-LEAP, Grant Number JP-MXS0118067246).

REFERENCES

- [1] Hanany, S., Niemack, M., and Page, L., "CMB Telescopes and Optical Systems," *Planets, Stars and Stellar Systems. Volume 1: Telescopes and Instrumentation* (06 2012).
- [2] Abitbol, M. H., Ahmed, Z., Barron, D., Thakur, R. B., Bender, A. N., Benson, B. A., Bischoff, C. A., Bryan, S. A., Carlstrom, J. E., Chang, C. L., Chuss, D. T., Crowley, K. T., Cukierman, A., de Haan, T., Dobbs, M., Essinger-Hileman, T., Filippini, J. P., Ganga, K., Gudmundsson, J. E., Halverson, N. W., Hanany, S., Henderson, S. W., Hill, C. A., Ho, S.-P. P., Hubmayr, J., Irwin, K., Jeong, O., Johnson, B. R., Kernasovskiy, S. A., Kovac, J. M., Kusaka, A., Lee, A. T., Maria, S., Mauskopf, P., McMahon, J. J., Moncelsi, L., Nadolski, A. W., Nagy, J. M., Niemack, M. D., O'Brient, R. C., Padin, S., Parshley, S. C., Pryke, C., Roe, N. A., Rostem, K., Ruhl, J., Simon, S. M., Staggs, S. T., Suzuki, A., Switzer, E. R., Tajima, O., Thompson, K. L., Timbie, P., Tucker, G. S., Vieira, J. D., Vieregg, A. G., Westbrook, B., Wollack, E. J., Yoon, K. W., Young, K. S., and Young, E. Y., "Cmb-s4 technology book, first edition," (2017).
- [3] Inoue, Y., Matsumura, T., Hazumi, M., Lee, A. T., Okamura, T., Suzuki, A., Tomaru, T., and Yamaguchi, H., "Cryogenic infrared filter made of alumina for use at millimeter wavelength," *Appl. Opt.* **53**, 1727–1733 (Mar 2014).
- [4] Lamb, J. W., "Miscellaneous data on materials for millimetre and submillimetre optics," *International Journal of Infrared and Millimeter Waves* 17 (12 1996).
- [5] Burgess, S. and Greig, D., "The low-temperature thermal conductivity of polyethylene," *Journal of Physics C: Solid State Physics* 8, 1637 (jun 1975).
- [6] Nemoto, T., Sasaki, S., and Hakuraku, Y., "Thermal conductivity of alumina and silicon carbide ceramics at low temperatures," *Cryogenics* **25**(9), 531–532 (1985).
- [7] Takaku, R., Wen, Q., Cray, S., Devlin, M., Dicker, S., Hanany, S., Hasebe, T., Iida, T., Katayama, N., Konishi, K., Kuwata-Gonokami, M., Matsumura, T., Mio, N., Sakurai, H., Sakurai, Y., Yamada, R., and Yumoto, J., "Large diameter millimeter-wave low-pass filter made of alumina with laser ablated anti-reflection coating," *Optics express* 29(25), 41745–41765 (2021).
- [8] Nadolski, A., Kofman, A. M., Vieira, J. D., Ade, P. A. R., Ahmed, Z., Anderson, A. J., Avva, J. S., Thakur, R. B., Bender, A. N., Benson, B. A., Carlstrom, J. E., Carter, F. W., Cecil, T. W., Chang, C. L., Cliche, J. F., Cukierman, A., de Haan, T., Ding, J., Dobbs, M. A., Dutcher, D., Everett, W., Foster, A., Fu, J., Gallichio, J., Gilbert, A., Groh, J. C., Guns, S. T., Guyser, R., Halverson, N. W., Harke-Hosemann, A. H.,

- Harrington, N. L., Henning, J. W., Holzapfel, W. L., Huang, N., Irwin, K. D., Jeong, O. B., Jonas, M., Jones, A., Khaire, T. S., Korman, M., Kubik, D. L., Kuhlmann, S., Kuo, C.-L., Lee, A. T., Lowitz, A. E., Meyer, S. S., Michalik, D., Montgomery, J., Natoli, T., Nguyen, H., Noble, G. I., Novosad, V., Padin, S., Pan, Z., Pearson, J., Posada, C. M., Quan, W., Rahlin, A., Ruhl, J. E., Sayre, J. T., Shirokoff, E., Smecher, G., Sobrin, J. A., Stark, A. A., Story, K. T., Suzuki, A., Thompson, K. L., Tucker, C., Vanderlinde, K., Wang, G., Whitehorn, N., Yefremenko, V., Yoon, K. W., and Young, M. R., "Broadband anti-reflective coatings for cosmic microwave background experiments," in [Millimeter, Submillimeter, and Far-Infrared Detectors and Instrumentation for Astronomy IX], Zmuidzinas, J. and Gao, J.-R., eds., 10708, 1070843, International Society for Optics and Photonics, SPIE (2018).
- [9] Groh, J. C., Design and Deployment of the Simons Array Cosmic Microwave Background Polarization Instrument, PhD thesis, University of California, Berkeley (Jan. 2021).
- [10] Ade, P. A. R., Ahmed, Z., Amiri, M., Barkats, D., Thakur, R. B., Bischoff, C. A., Beck, D., Bock, J. J., Boenish, H., Bullock, E., Buza, V., Cheshire IV, J. R., Connors, J., Cornelison, J., Crumrine, M., Cukierman, A., Denison, E. V., Dierickx, M., Duband, L., Eiben, M., Fatigoni, S., Filippini, J. P., Fliescher, S., Goeckner-Wald, N., Goldfinger, D. C., Grayson, J., Grimes, P., Hall, G., Halal, G., Halpern, M., Hand, E., Harrison, S., Henderson, S., Hildebrandt, S. R., Hilton, G. C., Hubmayr, J., Hui, H., Irwin, K. D., Kang, J., Karkare, K. S., Karpel, E., Kefeli, S., Kernasovskiy, S. A., Kovac, J. M., Kuo, C. L., Lau, K., Leitch, E. M., Lennox, A., Megerian, K. G., Minutolo, L., Moncelsi, L., Nakato, Y., Namikawa, T., Nguyen, H. T., OB'rient, R., Ogburn IV, R. W., Palladino, S., Prouve, T., Pryke, C., Racine, B., Reintsema, C. D., Richter, S., Schillaci, A., Schwarz, R., Schmitt, B. L., Sheehy, C. D., Soliman, A., Germaine, T. S., Steinbach, B., Sudiwala, R. V., Teply, G. P., Thompson, K. L., Tolan, J. E., Tucker, C., Turner, A. D., Umilta, C., Verges, C., Vieregg, A. G., Wandui, A., Weber, A. C., Wiebe, D. V., Willmert, J., Wong, C. L., Wu, W. L. K., Yang, H., Yoon, K. W., Young, E., Yu, C., Zeng, L., Zhang, C., and Zhang, S., "Bicep/keck xv: The bicep3 cosmic microwave background polarimeter and the first three-year data set," The Astrophysical journal 927(1), 77–(2022).
- [11] Ahmed, Z., Amiri, M., Benton, S. J., Bock, J. J., Bowens-Rubin, R., Buder, I., Bullock, E., Connors, J., Filippini, J. P., Grayson, J. A., Halpern, M., Hilton, G. C., Hristov, V. V., Hui, H., Irwin, K. D., Kang, J., Karkare, K. S., Karpel, E., Kovac, J. M., Kuo, C. L., Netterfield, C. B., Nguyen, H. T., O'Brient, R., IV, R. W. O., Pryke, C., Reintsema, C. D., Richter, S., Thompson, K. L., Turner, A. D., Vieregg, A. G., Wu, W. L. K., and Yoon, K. W., "BICEP3: a 95GHz refracting telescope for degree-scale CMB polarization," in [Millimeter, Submillimeter, and Far-Infrared Detectors and Instrumentation for Astronomy VII], Holland, W. S. and Zmuidzinas, J., eds., 9153, 91531N, International Society for Optics and Photonics, SPIE (2014).
- [12] Sakaguri, K., Hasegawa, M., Sakurai, Y., Hill, C., and Kusaka, A., "Broadband multi-layer anti-reflection coatings with mullite and duroid for half-wave plates and alumina filters for cmb polarimetry," *Journal of Low Temperature Physics* **209**, 1264–1271 (Dec 2022).
- [13] Golec, J. E., Sutariya, S., Jackson, R., Zimmerman, J., Dicker, S. R., Iuliano, J., McMahon, J., Puglisi, G., Tucker, C., and Wollack, E. J., "Simons observatory: broadband metamaterial antireflection cuttings for large-aperture alumina optics," Appl. Opt. 61, 8904–8911 (Oct 2022).
- [14] Nadolski, A., Vieira, J. D., Sobrin, J. A., Kofman, A. M., Ade, P. A. R., Ahmed, Z., Anderson, A. J., Avva, J. S., Thakur, R. B., Bender, A. N., Benson, B. A., Bryant, L., Carlstrom, J. E., Carter, F. W., Cecil, T. W., Chang, C. L., Cheshire, J. R., Chesmore, G. E., Cliche, J. F., Cukierman, A., de Haan, T., Dierickx, M., Ding, J., Dutcher, D., Everett, W., Farwick, J., Ferguson, K. R., Florez, L., Foster, A., Fu, J., Gallicchio, J., Gambrel, A. E., Gardner, R. W., Groh, J. C., Guns, S., Guyser, R., Halverson, N. W., Harke-Hosemann, A. H., Harrington, N. L., Harris, R. J., Henning, J. W., Holzapfel, W. L., Howe, D., Huang, N., Irwin, K. D., Jeong, O., Jonas, M., Jones, A., Korman, M., Kovac, J., Kubik, D. L., Kuhlmann, S., Kuo, C.-L., Lee, A. T., Lowitz, A. E., McMahon, J., Meier, J., Meyer, S. S., Michalik, D., Montgomery, J., Natoli, T., Nguyen, H., Noble, G., Novosad, Padin, S., Pan, Z., Paschos, P., Pearson, J., Posada, C. M., Quan, W., Rahlin, A., Riebel, D., Ruhl, J. E., Sayre, J., Shirokoff, E., Smecher, G., Stark, A. A., Stephen, J., Story, K. T., Suzuki, A., Tandoi, C., Thompson, K. L., Tucker, C., Vanderlinde, K., Wang, G., Whitehorn, N., Yefremenko, Yoon, K. W., and Young, M. R., "Broadband, millimeter-wave antireflection coatings for large-format, cryogenic aluminum oxide optics," Applied optics (2004) 59(10), 3285–3295 (2020).

- [15] M., R. S., "Electromagnetic properties of a finely stratified medium," Sov. Phys. JEPT Engl. Transl. 2, 466–475 (1956).
- [16] Shabat, M. M. and Ubeid, M. F., "Antireflection coating at metamaterial waveguide structures for solar energy applications," *Energy Procedia* 50, 314–321 (2014). Technologies and Materials for Renewable Energy, Environment and Sustainability (TMREES14 – EUMISD).
- [17] Chen, H.-T., Zhou, J., O'Hara, J. F., Chen, F., Azad, A. K., and Taylor, A. J., "Antireflection coating using metamaterials and identification of its mechanism," *Phys. Rev. Lett.* **105**, 073901 (Aug 2010).
- [18] Jeon, J., Bhattarai, K., Kim, D.-K., Kim, J. O., Urbas, A., Lee, S. J., Ku, Z., and Zhou, J., "A low-loss metasurface antireflection coating on dispersive surface plasmon structure," *Scientific Reports* 6, 36190 (Nov 2016).
- [19] Matsumura, T., Young, K., Wen, Q., Hanany, S., Ishino, H., Inoue, Y., Hazumi, M., Koch, J., Suttman, O., and Schütz, V., "Millimeter-wave broadband antireflection coatings using laser ablation of subwavelength structures," *Appl. Opt.* **55**, 3502–3509 (May 2016).
- [20] Schütz, V., Young, K., Matsumura, T., Hanany, S., Koch, J., Suttmann, O., Overmeyer, L., and Wen, Q., "Laser processing of sub-wavelength structures on sapphire and alumina for millimeter wavelength broadband anti-reflection coatings," *Journal of Laser Micro Nanoengineering* 11, 204–209 (01 2016).
- [21] Young, K., Wen, Q., Hanany, S., Imada, H., Koch, J., Matsumura, T., Suttmann, O., and Schütz, V., "Broadband millimeter-wave anti-reflection coatings on silicon using pyramidal sub-wavelength structures," *Journal of Applied Physics* **121** (6 2017).
- [22] Matsumura, T., Takaku, R., Hanany, S., Imada, H., Ishino, H., Katayama, N., Kobayashi, Y., Komatsu, K., Konishi, K., Kuwata-Gonokami, M., Nakamura, S., Sakurai, H., Sakurai, Y., Wen, Q., Young, K., and Yumoto, J., "Prototype demonstration of the broadband anti-reflection coating on sapphire using a sub-wavelength structure," in [29th IEEE International Symposium on Space Terahertz Technology, ISSTT 2018], 54-60 (Jan. 2018). 29th IEEE International Symposium on Space Terahertz Technology, ISSTT 2018; Conference date: 26-03-2018 Through 28-03-2018.
- [23] Takaku, R., Hanany, S., Imada, H., Ishino, H., Katayama, N., Komatsu, K., Konishi, K., Kuwata-Gonokami, M., Matsumura, T., Mitsuda, K., Sakurai, H., Sakurai, Y., Wen, Q., Yamasaki, N. Y., Young, K., and Yumoto, J., "Broadband, millimeter-wave anti-reflective structures on sapphire ablated with femto-second laser," *Journal of Applied Physics* 128(22), 225302 (2020).
- [24] Takaku, R., Hanany, S., Hoshino, Y., Imada, H., Ishino, H., Katayama, N., Komatsu, K., Konishi, K., Gonokami, M. K., Matsumura, T., Mitsuda, K., Sakurai, H., Sakurai, Y., Wen, Q., Yamasaki, N. Y., Young, K., and Yumoto, J., "Demonstration of anti-reflective structures over a large area for cmb polarization experiments," in [Millimeter, Submillimeter, and Far-Infrared Detectors and Instrumentation for Astronomy X], Zmuidzinas, J. and Gao, J.-R., eds., 11453, 236 247, International Society for Optics and Photonics, SPIE (2020).
- [25] Takaku, R., Azzoni, S., Ghigna, T., Hasebe, T., Hoang, T. D., Hoshino, Y., Katayama, N., Komatsu, K., Konishi, K., Kuwata-Gonokami, M., Matsumura, T., Sakurai, H., Sakurai, Y., Sugiyama, S., Yamasaki, N. N., and Yumoto, J., "Impact of the effective thickness from anti-reflective sub-wavelength structures in achromatic half-wave plate design," in [Millimeter, Submillimeter, and Far-Infrared Detectors and Instrumentation for Astronomy XI], Zmuidzinas, J. and Gao, J.-R., eds., 12190, 121902K, International Society for Optics and Photonics, SPIE (2022).
- [26] Takaku, R., Ghigna, T., Hanany, S., Hoshino, Y., Ishino, H., Katayama, N., Komatsu, K., Konishi, K., Kuwata-Gonokami, M., Matsumura, T., Sakurai, H., Sakurai, Y., Wen, Q., Yamasaki, N. Y., Yumoto, J., and for the LiteBIRD collaboration, "Performance of a 200 mm diameter achromatic hwp with laser-ablated sub-wavelength structures," Journal of Low Temperature Physics 211, 346–356 (Jun 2023).
- [27] Masi, S., Battistelli, E., de Bernardis, P., Coppolecchia, A., Columbro, F., D'Alessandro, G., De Petris, M., Lamagna, L., Marchitelli, E., Mele, L., Paiella, A., Piacentini, F., Pisano, G., Bersanelli, M., Franceschet, C., Manzan, E., Mennella, D., Realini, S., Cibella, S., Martini, F., Pettinari, G., Coppi, G., Gervasi, M., Limonta, A., Zannoni, M., Piccirillo, L., and Tucker, C., "The cosmic monopole observer (cosmo)," arXiv (Cornell University) (2021).

- [28] Wen, Q., Fadeeva, E., Hanany, S., Koch, J., Matsumura, T., Takaku, R., and Young, K., "Picosecond laser ablation of millimeter-wave subwavelength structures on alumina and sapphire," *Optics & Laser Technology* **142**, 107207 (2021).
- [29] https://www.ansys.com/campaigns/ansys-best-in-class-electromagnetic-simulation-software.